horticulturae

MDPI

Article

Transcriptome Profiling Reveals Potential Genes Involved in Salicylic Acid-Induced Arbutin Synthesis in Pear

Junhao Li [1,2], Yuchen Ma [2], Tingting Cui [2], Shaohua Liu [2] and Liulin Li [2,*]

[1] Shijiazhuang Institute of Fruit Trees, Hebei Academy of Agriculture and Forestry, Shijiazhuang 050061, China; sxtgljh@163.com
[2] College of Horticulture, Shanxi Agricultural University, Taigu, Jinzhong 030801, China
* Correspondence: tgliulin@163.com; Tel.: +86-03-54-62-859-08

Abstract: Salicylic acid (SA) is known to be an efficient elicitor of secondary metabolism in plants. Arbutin, a characteristic phenolic glycoside found in 'Yuluxiang' pear (*Pyrus bretschneideri* Rehder × *Pyrus sinkiangensis* Yu), is widely used in lightening agents, in addition to cough, anti-inflammatory, and anti-microbial remedies, among other applications. However, research into the synthesis of arbutin in pear is limited. This study aimed to clarify the effect of exogenous SA on the arbutin content of pear using HPLC and investigate the mechanism for arbutin accumulation using RNA-Seq analysis. HPLC revealed that SA increased the arbutin contents of leaf, fruit, and callus in pear and demonstrated that the effect of SA is concentration and time dependent. RNA-Seq analysis of pear callus treated with or without SA revealed 380 differentially expressed genes (DEGs), 335 of which were up-regulated. According to a KEGG database analysis, the highest number of genes were annotated for phenylpropane biosynthesis. Overall, 21 DEGs were found to be involved in the synthesis of hydroquinone and UDP-glucose, which are substrates of arbutin synthesis. It is noteworthy that the expression levels of three up-regulated genes (*Pbr006844.1*, *Pbr021064.1* and *Pbr021069.1*) related to hydroquinone glycosyltransferase were induced by SA and hydroquinone. Furthermore, transient overexpression of *PbUGT72B1* (*Pbr021069.1*) increased the arbutin content in pear callus. These data explain the regulation of gene transcription associated with the promotive effect of SA on arbutin biosynthesis in pear, thus providing a theoretical foundation for enhancing the arbutin content of fruit through genetic engineering.

Keywords: pear; arbutin; salicylic acid; transcriptome; UGT

check for updates

Citation: Li, J.; Ma, Y.; Cui, T.; Liu, S.; Li, L. Transcriptome Profiling Reveals Potential Genes Involved in Salicylic Acid-Induced Arbutin Synthesis in Pear. *Horticulturae* **2024**, *10*, 622. https://doi.org/10.3390/horticulturae10060622

Academic Editors: Adriana F. Sestras and Zhenchang Liang

Received: 2 March 2024
Revised: 26 May 2024
Accepted: 3 June 2024
Published: 11 June 2024

Copyright: © 2024 by the authors. Licensee MDPI, Basel, Switzerland. This article is an open access article distributed under the terms and conditions of the Creative Commons Attribution (CC BY) license (https://creativecommons.org/licenses/by/4.0/).

1. Introduction

Pear, of the family Rosaceae, is the third most widely grown temperate fruit tree species in the world [1]. Pear fruits have been consumed as a healthy food product and used in traditional medicines for more than two millennia [2]. Their efficacy in relieving fever, cough, urinary disorders, and alcohol-induced hangovers was widely recorded in ancient medicinal prescriptions found in China, Japan, and Korea. These functional characteristics of pear have, over time, been supported by scientific evidence [3]. In addition, the medicinal functions of pear are constantly being explored. For example, Navaei et al. found that daily fresh pear consumption may promote modest improvements in the cardiometabolic health of middle-aged/older adults with metabolic syndrome, a function that correlates strongly with the nutritional components of these fruits [4,5].

Arbutin (hydroquinone-β-D-glucopyranoside), the most abundant phenolic glycoside in pear, is used as a biomarker for pear intake [6,7]. It is widely used in the cosmetics industry, owing to the ability of tyrosinase to block melanin synthesis [8]. Arbutin is believed to have a variety of health benefits. Some studies have suggested that arbutin from different parts of the pear exhibits anti-inflammatory effects on pro-inflammatory cytokines such as IL-1β, TNF-α, and MCP-1, which are attributed to the cytokine storm of

COVID-19 [9–11]. Nahar et al. suggested its potential substance as an anticancer agent [12]. Jurica et al. proposed that hydroquinone, a metabolite of arbutin, has strong antimicrobial activity against some uropathogens [13], while others have found that it suppresses angular leaf spot disease [14]. Moreover, some studies have indicated that in plants, arbutin plays an important role in resistance to abiotic stress. For example, Wei et al. found that arbutin was correlated to the drought resistance of *Carthamus tinctorius* L. [15]. Lawas et al. also suggested that Dular, the drought-tolerant variety, exhibited the highest constitutive levels of arbutin compared with Anjali [16]. Therefore, it is significant to elucidate the metabolic mechanism of arbutin. In 1960, Grisdale and Towers found that arbutin is synthesized from shikimic acid and phenylpropanoid compounds in *P. communis* [17]. In addition, only hydroquinone glucosyltransferase from *Rauvolfia* was identified to be involvemed in the synthesis of arbutin [18,19].

Salicylic acid (SA) is an important signaling molecule that has received a high level of attention from researchers worldwide [20]. SA is reported to be involved in diverse plant growth and development responses and to affect the maturity, quality, and senescence of fruit. Importantly, these functions are closely related to changes in secondary metabolic activities. For example, SA can increase the decay rate of apricots and goji berries by regulating phenol metabolism [21,22]. In recent years, the impact of SA on secondary metabolite accumulation in different plant species has been the focus of numerous studies. As an efficient elicitor, SA treatment increases the terpene trilactone content in Ginkgo biloba [23] and the sulforaphane content of radish taproot [24], although with no significant change in glucosinolate. In pear, SA has been noted to delay fruit ripening and senescence by regulating genes associated with plant hormone biosynthesis and metabolism, cell wall metabolism and modification, antioxidant systems, and the biosynthesis of esters [25,26]. However, little is known about the effects of SA treatment on arbutin biosynthesis in pear.

Recently, transcriptomics has become a primary tool for determining the regulatory mechanisms associated with the active ingredients of medicinal plants, revealing biosynthetic pathways, and identifying key genes involved in secondary metabolism. In order to explore arbutin content following application of salicylic acid and the biosynthesis molecular mechanism of arbutin, we first investigated the effects of SA on the arbutin content in 'Yuluxiang' pear (*P. bretschneideri* Rehder × *P. sinkiangensis* Yu) using high-performance liquid chromatography (HPLC) and screened differentially expressed (DEGs) associated with arbutin biosynthesis using transcriptome analysis to identify key arbutin biosynthesis genes. Additionally, we cloned, expressed, and characterized hydroquinone glycosyltransferase (*PbUGT72B1*), which is related to arbutin glycosylation. The results provide a foundation for understanding the role of SA in arbutin biosynthesis and exploring the molecular mechanism of arbutin biosynthesis in pear.

2. Materials and Methods

2.1. Plant Material

Leaves and fruits of pear variety 'Yuluxiang' (*P. bretschneideri* Rehder × *P. sinkiangensis* Yu) were obtained from the Pomology Institute of Shanxi Agricultural University, Shanxi Province, China (112.5°, 37.3°) in 2021. Callus formation was induced on 'Yuluxiang' fruits following the method described by Zhao et al. [27]. Surface stains were removed using detergent; then, fruits were disinfected with 75% ethanol for 40 s and 0.1% $HgCl_2$ for 20 min. The peel was removed with a sterile scalpel, and the flesh was cut into small pieces (10 × 10 mm) before inoculation onto MS solid medium (AA949, BINDE, Qingdao, China) supplemented with 0.5 mg·L^{-1} 6-benzylaminopurine (6-BA), 2.0 mg·L^{-1} 2,4-dichlorophenoxyacetic acid (2,4-D), 0.6% (w·v^{-1}) agar and 3% (w·v^{-1}) sucrose at a pH of 5.8. The induced calli were transferred to solid media containing MS, 1.0 mg·L^{-1} 6-BA, and 1.5 mg·L^{-1} 2,4-D for subculture once every 15 days.

2.2. SA Treatments

SA was dissolved in 98% ethanol to produce a 1 mM solution, which was diluted to final concentrations of 50, 100, 150, and 200 μM with ultra-pure water. The SA treatments or a control solution (distilled water) were applied exogenously by spraying the annual shoots or fruits in May 2021. The fifth leaf from the shoot apex and fruits from three randomly selected individuals were collected every 24 h, respectively. To treat the pear calli, 200 μL of the SA working solution was placed on the surface of solid MS medium using a pipette and spread evenly with a spreading rod. Callus not treated with SA was used as control. The calli were sampled after 6, 12, 24, 48, and 72 h. One petri dish was considered a biological replicate and repeated three times. All samples were immersed in liquid nitrogen and stored at −80 °C for further analysis.

2.3. Hydroquinone Treatments

Hydroquinone treatments were conducted following the method described by Skrzypczak-Piekoszewska et al. [28]. with minor modifications. Fifty milliliters of fresh media were added to each petri dish. Hydroquinone (≥98%) was purchased from Shanghai yuanye Bio-Technology Co., Ltd (Shanghai, China). It was dissolved in water and added to MS medium to produce final hydroquinone concentrations of 220, 440, 660, 880, or 1100 mg L^{-1}. The hydroquinone was added in a single dose or doses divided into two or three portions. One week after inoculation, callus growth was measured, and the samples were frozen in liquid nitrogen.

2.4. Measurement of Arbutin Content

The method used to measure arbutin content was as described by Cui et al. [29]. Frozen samples were homogenized in methanol solution (70%) and incubated in an ultrasonic oscillator (DT 512 H, BANDELIN, Berlin, Germany) for 20 min. After centrifugation at 5000 rpm for 20 min at 4 °C, the supernatant was collected and filtered through a 0.22 μm membrane filter (JINTENG, Tianjin, China). The HPLC system (Agilent 1260, Santa Clara, CA, USA) used to determine the arbutin content of the filtrate was equipped with a diode array detector set to 30 °C and a Venusil ASB C18 column (4.6 mm × 250 mm × 5 μm, Agela Technologies, Tianjin, China). The mobile phase consisted of A: 5% formic acid and B: acetonitrile solution at a flow rate of 0.8 mL min^{-1}. The gradient elution was as follows: 10–13% B for 5 min, 13–16% B for 20 min, 16–21% B for 5 min, and 10% B for 3 min. Dose-dependent calibration curves of arbutin standards were established, and the concentrations of arbutin were quantified using the standard curves. Arbutin (≥98%) was purchased from Shanghai Yuanye Bio-Technology Co., Ltd (Shanghai, China).

2.5. RNA Extraction, cDNA Library Construction, and Sequencing

Two samples (CK_24 h and SA_24 h) were used for RNA-seq. Total RNA was extracted using the Trizol method, and the concentration and purity of the RNA were measured using a NanoDrop 2000 spectrophotometer (Thermo Fisher Science, Wilmington, DE, USA). RNA integrity was evaluated using an Agilent Biological Analyzer 2100 system (Agilent Technologies, Santa Clara, CA, USA). Sequencing libraries were generated using a VAHTS mRNA-seq V3 Library Prep Kit for Illumina (Vazyme, Nanjing, China) following the manufacturer's recommendations. The primary sequencing data were filtered for quality control to obtain clean data. Then, the clean reads were aligned to the reference genome (http://peargenome.njau.edu.cn/allfile/4.Pyrus_bretschneideri_scaffold.gz, accessed on 11 October 2021). To classify genes into functional categories, the assembled genes or transcripts were functionally annotated by mapping to the six public databases, including NR, Swiss-Prot, Pfam, STRING, GO and KEGG. Finally, gene expression values were calculated with the Fragments Per Kilobase of transcript per the million mapped reads (FPKM) method, and genes fulfilling the criteria of $|\log2 \text{ (fold change)}| \geq 2$ and false discovery rate < 0.05 obtained by DESeq2 were considered to be DEGs.

2.6. Quantitative Real-Time PCR Analysis

Seventeen genes were selected for quantitative real-time (qRT)-PCR analysis. cDNA was synthesized using a PrimeScript™ RT reagent kit with gDNA Eraser (TaKaRa, Dalian, China) according to the manufacturer's instructions. A ChamQ Universal SYBR qPCR Master Mix Kit (Vazyme, Nanjing, China) and a LightCycler96 Real-Time system (Rache, Basel, Switzerland) were used to complete the qRT-PCR. The relative expression of each gene was calculated according to the $2^{-\Delta\Delta CT}$ method. Gene-specific primers were designed using Primer 5.0, and these are listed in Table S1.

2.7. Transient Transformation of PbUGT72B1 into Pear

To verify the gene function of *PbUGT72B1*, we amplified and cloned the full length of *Pbr021069.1*, named *PbUGT72B1,* according to phylogenetic analysis. The recombined pBWA(V)BS-PbUGT72B1 vector was constructed and transformed into Agrobacterium tumefaciens strain GV3101 using the free-thaw method for transient infection. GV3101 cells containing the PbUGT72B1 constructs and the empty vector were cultured in LB liquid medium (2 mL) comprising 20 mg·L^{-1} rifampicin and 50 mg·L^{-1} kanamycin at 28 °C. The bacterial solution was transferred into 40 mL of LB liquid medium for culture. Next, the bacterial solution was collected, resuspended with osmotic suspension (10 mmol·L^{-1} MES, 10 mmol·L^{-1} $MgCl_2$, 150 μmol·L^{-1} ACE, pH 5.6), and adjusted to an optical density (OD600) of 0.3. Calli were immersed in this solution, and vacuum infiltration (SHZ-III, Shanghai, China) was conducted for 15 min. The calli were rinsed three times with sterile water and cultured on MS medium with or without hydroquinone (50 mg·L^{-1}) for 3 days.

2.8. Statistical Analysis

The significance of the data differences was statistically analyzed by one-way analysis of variance (ANOVA) using SAS V8 software (SAS Inc., Cary, NC, USA). Duncan's test was used to assess statistical differences ($p < 0.05$).

3. Results

3.1. Arbutin Contents of Pear Leaves Treated with SA

As shown in Figure 1, the arbutin contents of leaves were considerably affected by SA treatment. Following 1 day of treatment with SA at 100, 150, and 200 μM, respectively, arbutin contents were found to decrease. However, following 2- and 3-day treatments with 50, 100, and 200 μM SA, respectively, the arbutin contents were higher than that of the CK. The arbutin content was highest after 4 days of treatment with 50 and 100 μM SA, respectively, while treatment with 200 μM SA resulted in the lowest arbutin levels. The 5-day treatment with SA did not significantly influence the arbutin content compared with the CK.

3.2. Arbutin Contents of Fruits Treated with SA

As depicted in Figure 2, SA had a significant effect on the arbutin contents of pear fruits. After treatment with 150 μM SA, the arbutin content reached its highest levels after 1 and 2 days. However, the arbutin contents were lowest after the 3-day treatments with 100 and 150 μM SA, respectively. After 5 days, treatment with 150 μM SA resulted in a higher arbutin content compared with the other treatments and the control.

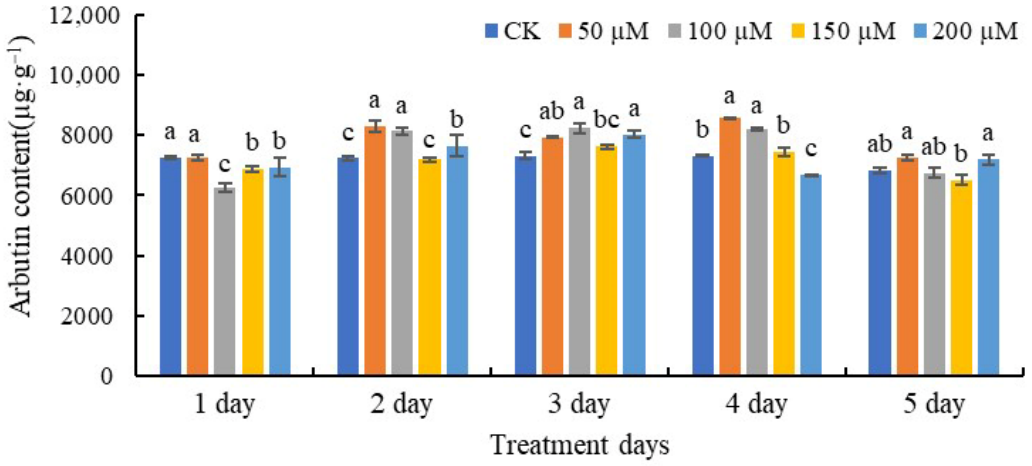

Figure 1. The contents of arbutin in leaves treated with SA. Each data point represents the mean of three independent replicates (mean ± SE). The values with different letters indicate significant differences among the treatments containing different concentrations of SA at one point of time at $p < 0.05$.

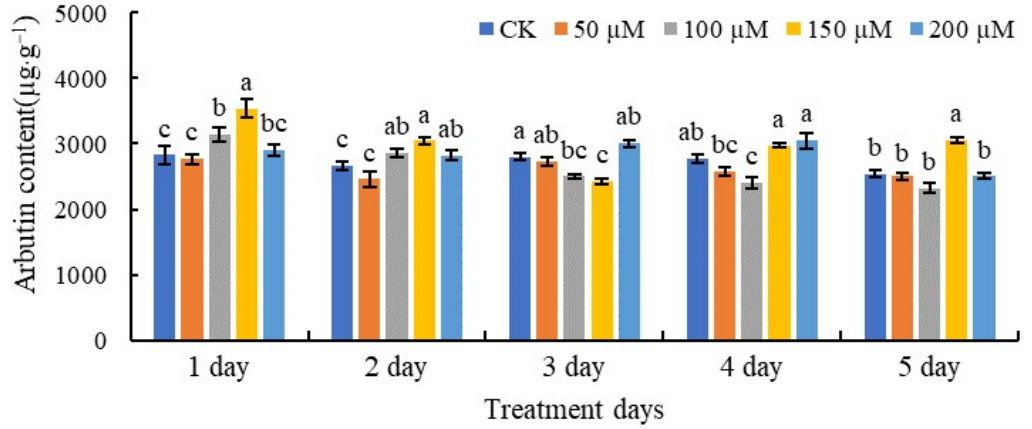

Figure 2. The contents of arbutin in pear fruits treated with SA. The values with different letters indicate significant differences among the treatments containing different concentrations of SA at one point of time at $p < 0.05$.

3.3. Arbutin Contents of Calli Treated with SA

The changes in the arbutin contents of pear callus after SA treatment are shown in Figure 3. After 6 h of SA treatment, the arbutin content only increased significantly at an SA concentration of 200 μM compared with the control. The content of arbutin was highest in pear callus treated with 100 μM SA for 12 h. Compared with the control at 24 h and 48 h, different concentrations of SA induced the accumulation of arbutin. In detail, after treatment with 50, 100, 150, and 200 μM SA for 24 h, the arbutin contents were 1.28-fold, 2.07-fold, 1.58-fold, and 1.63-fold higher than those of the control callus, respectively. After 48 h of application of 50 and 200 μM, SA resulted in the highest level of arbutin—1.71-fold higher than that of the control. The arbutin content showed no significant difference among calli treated with 50, 100, or 200 μM SA for 72 h, but the arbutin levels following these treatments were all higher than those of the control after 72 h.

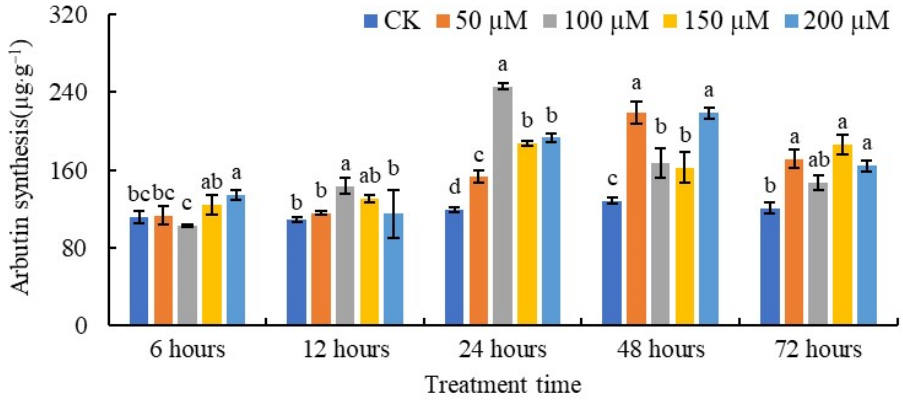

Figure 3. The content of arbutin in pear callus under SA treatment. The values with different letters indicate significant differences among the treatments containing different concentrations of SA at one point of time at $p < 0.05$.

3.4. RNA-Seq of Pear Callus under SA Treatment

To investigate the molecular mechanisms of arbutin biosynthesis regulated by SA and mine the genes associated with arbutin in pear, calli from the 24 h control and 100 μM SA treatments were collected for transcriptome sequencing. As shown in Table S2, at least 38,279,434 clean reads were obtained in each library after removing the low-quality reads, and GC percentages ≥ 47.38% and Q30 values ≥ 94.69% were obtained. The total of the mapped reads was >73.05%. These results indicated that the transcriptome data were suitable for use in further analyses.

All of the assembled genes were annotated to the eight public databases. The results in Table S3 show that 43,922 genes were annotated in the NR database, 38,570 in the eggNOG database, 33,501 in the GO database, 32,206 in the Pfam database, 28,864 in the Swiss-Prot database, 28,483 in the KEGG database, 21,259 in the KOG database, and 13,079 in the COG database.

3.5. Analysis of DEGs in Response to SA

Two libraries (control and SA treatment) were constructed for pairwise comparison analysis to identify the DEGs. As shown in Figure 4, 380 DEGs were identified, with 335 up-regulated and 45 down-regulated. Fifteen DEGs were selected for qRT-PCR analysis to evaluate the quality of the RNA-seq data. The expression patterns of the 15 selected genes obtained from RNA-Seq and qRT-PCR were found to be consistent (Figure S2), with a Pearson coefficient of 0.813. The results demonstrated that the transcriptome sequencing data were reliable and that the RNA-Seq results were of high quality and suitable for further analysis.

3.6. Functional Analysis of DEGs

To better characterize the functions of genes that were differentially expressed between the CK and SA-treated calli, COG, GO, and KEGG enrichment analyses were completed. Overall, 152 DEGs were annotated in the COG database, and these genes were enriched for 19 COG items as shown in Figure S1. The results indicated that 29 DEGs were involved in secondary metabolite biosynthesis, transport and catabolism (Q) and 25 were involved in carbohydrate transport and metabolism (G), while 19 were related to signal transduction mechanisms (T). As revealed in Figure S2, 321 DEGs were annotated in the GO database, with 12 enriched for cellular components, 11 for molecular function, and 15 for biological processes. The DEGs associated with cellular components were composed mainly of membrane (103 genes) and membrane parts (99 genes). DEGs for molecular function were mainly related to catalytic activity (181 genes) and binding (50 genes). Genes involved in biological processes were mainly associated with the regulation of the metabolic process (132 genes), the single-organism process (95 genes), and the cellular process (93 genes). In a

more detailed investigation into DEG function, pathway annotations of DEGs using the KEGG database revealed that most DEGs were enriched in KEGG terms for plant–pathogen interaction (ko04626, 25 genes) and phenylpropanoid biosynthesis (ko00940, 23 genes) (Figure S3). The top 20 significantly enriched pathways were further screened (Figure 5), and the results indicated that the q-value of phenylpropanoid biosynthesis was the highest.

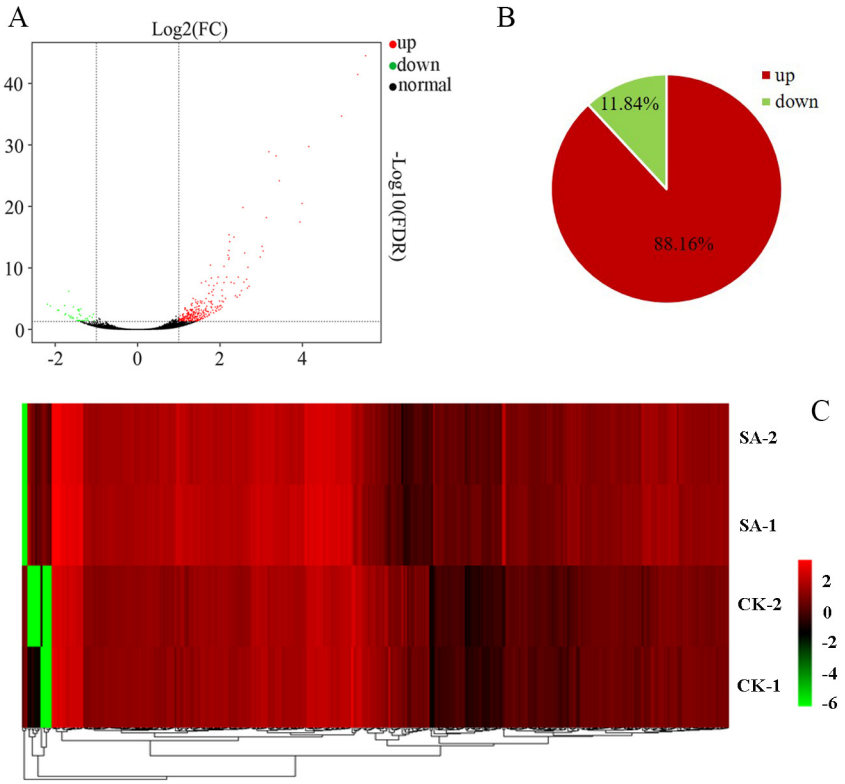

Figure 4. DEGs in the control (CK) and SA-treated calli. (**A**) MA plot of DEGs, each dot in the MA map of DEGs represented a gene. (**B**) Proportions of up- and down-regulated DEGs. (**C**) Heatmap presentation of fold changes (FC) in 380 DEGs obtained from RNA-seq analysis. SA-1 and SA-2 represented two biological replicates of 100 μM SA treatment, CK-1 and CK-2 represented two biological replicates of distilled water treatment. And each biological replicate sample comes from a mixture of callus samples cultivated in three culture dishes.

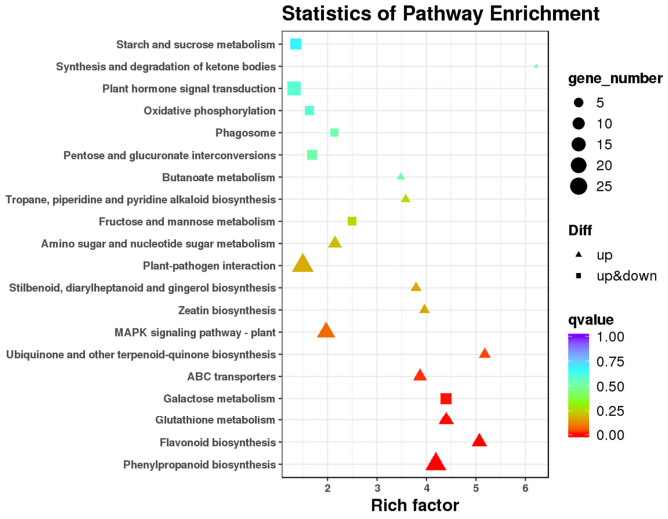

Figure 5. Top 20 KEGG enrichment classifications of DEGs in response to SA treatment.

3.7. Key Genes in the Arbutin Biosynthesis Pathway

It has been reported that arbutin is a type of phenolic glycoside. Therefore, we searched arbutin biosynthetic pathway genes, as seen in Figure 6. The substance hydroquinone is produced via phenylpropanoid biosynthesis and tyrosine metabolism. In phenylpropanoid biosynthesis, the transcript abundance of five genes, including *Pbr008363.1*, *Pbr013141.1*, *Pbr017290.1*, *Pbr036272.1*, and *Pbr039972.1*, was significantly increased after exposure to SA. Meanwhile, only one gene (*Pbr008105.1*) involved in tyrosine metabolism was expressed at a significantly higher level under the SA treatment than in the control. UDP-glucose, as a glucosyl donor, provides glucose to generate arbutin. With reference to Figure 6, the DEGs enriched in amino sugar and nucleotide sugar metabolism (ko00520), pentose and glucuronate interconversion (ko00040), galactose metabolism (ko00052), and starch and sucrose metabolism (ko00500) participate in the synthesis of UDP-glucose. In ko00520, the expression levels of four genes (*Pbr010819.1*, *Pbr034281.1*, *Pbr037930.1*, and *Pbr037931.1*) were up-regulated under SA treatment. In ko00040, the expression levels of four genes (*Pbr038705.1*, *Pbr037379.1*, *Pbr035887.1*, and *Pyrus_x_bretschneideri_newGene_11219*) were up-regulated under SA treatment. In ko00052, the expression level of *Pbr034089.1* was down-regulated under SA treatment, along with *Pyrus_x_bretschneideri_newGene_11219*, also associated with the metabolic process. In ko00500, a total of six DEGs were identified in callus exposed to SA, and only *Pbr038578.1* was down-regulated.

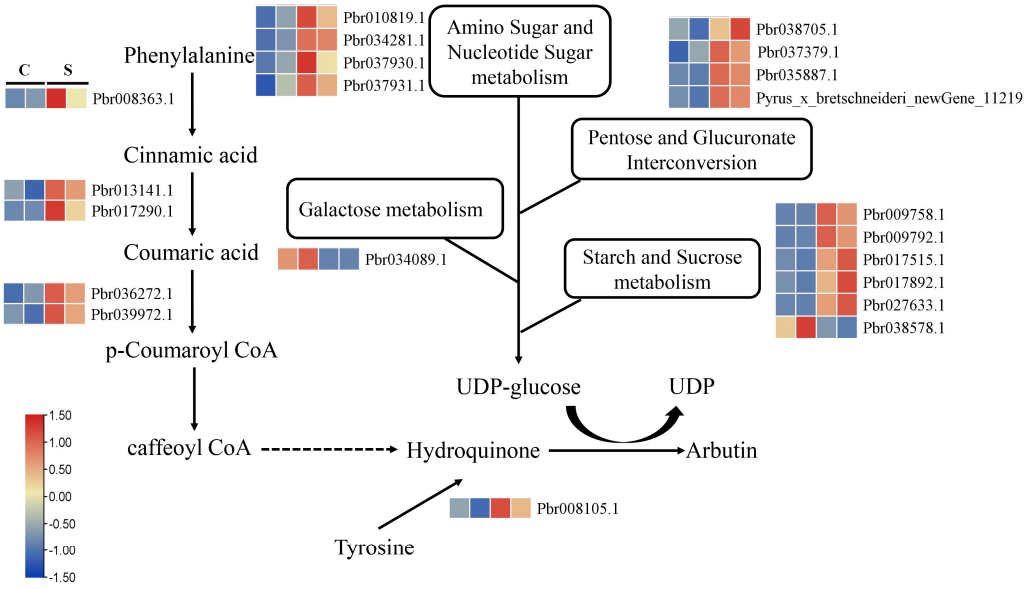

Figure 6. Expression patterns of DEGs involved in a proposed pathway of arbutin biosynthesis.

Glycosylation is the last step in arbutin synthesis. A total of 15 DEGs encoding glycosyltransferase were identified in callus exposed to SA (Figure 7). Among them, only the expression level of *Pbr034061.1* was down-regulated under SA treatment. According to the Pfam annotation, 11 DEGs associated with UDP-glucosyl transferase, particularly *Pbr006844.1*, *Pbr021064.1* and *Pbr021069.1*, were predicted to be hydroquinone glucosyltransferase-like. These three genes may therefore be involved in the process of arbutin glycosylation.

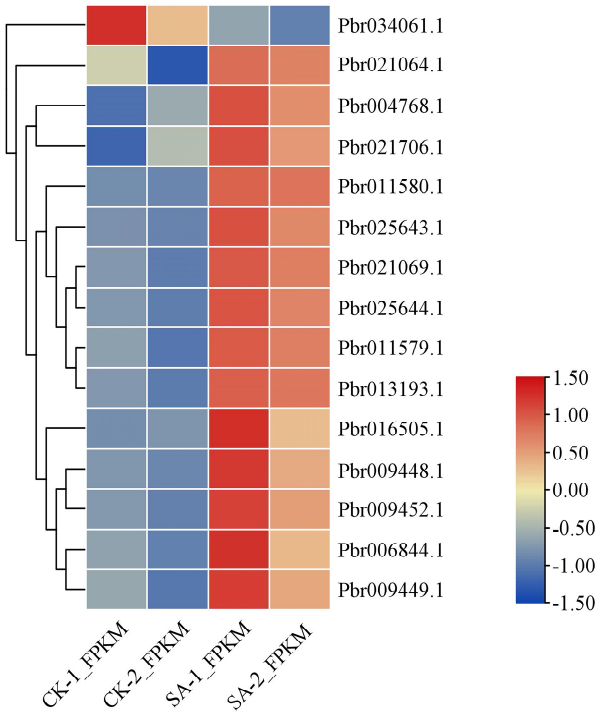

Figure 7. Expression profiles of DEGs related to glycosyltransferase.

3.8. Transcription Factor Responses to SA Treatment

It is well known that transcription factors play important roles in the regulation of secondary metabolism. In this study, a total of 18 differentially expressed transcription factors were screened under SA treatment as shown in Figure 8. These were classified into five subfamilies according to their protein domains, including ERF, WRKY, bHLH, MYB, and NAC. Of the 18 transcription factors screened, only *Pbr038280.1* was down-regulated.

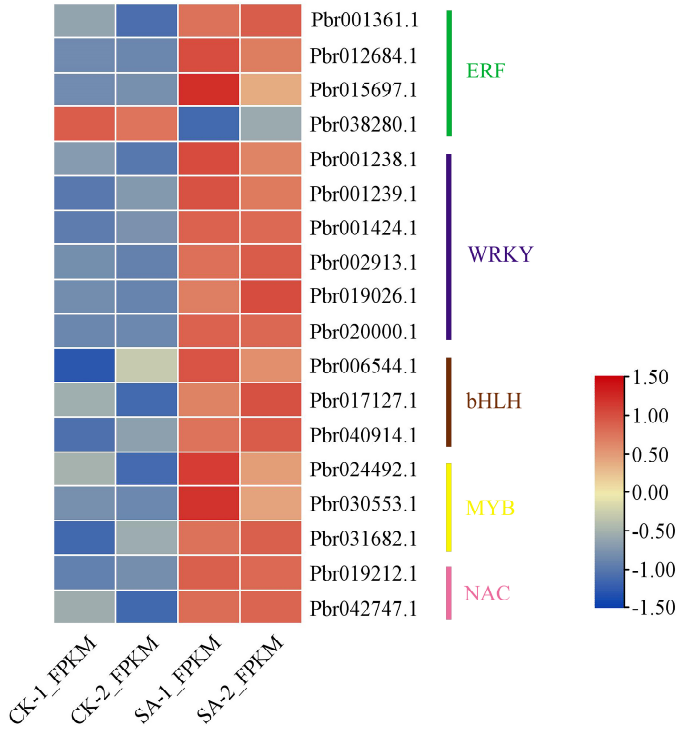

Figure 8. Expression profiles of transcription factors among the DEGs identified under SA treatment.

3.9. Effect of Hydroquinone Feeding on Arbutin Content and Gene Expression

In this study, the precursor, hydroquinone, was supplemented to explore its effect on arbutin content. As shown in Table S4, hydroquinone supplementation had an adverse effect on the growth of the calli compared with the control. The application of divided doses of hydroquinone reduced its negative effect on callus growth. Compared with other hydroquinone treatments, the growth rate was highest when the precursor concentration was 220 mg·L^{-1} and it was added in three portions. However, the arbutin content increased significantly when hydroquinone was added to the callus cultures. The arbutin content was highest (5093.93 μg·g^{-1}) when the precursor was added at a concentration of 660 mg·L^{-1} in one undivided dose, whereas the arbutin content was highest (4880.20 μg·g^{-1}) when the precursor was added at a concentration of 880 mg·L^{-1} in two portions. The highest arbutin concentration (2969.95 μg·g^{-1}) was obtained when the precursor concentration was 1100 mg·L^{-1}, and it was added in three portions.

From transcriptome data, except for the three genes (*Pbr006844.1*, *Pbr021064.1* and *Pbr021069.1*) encoding hydroquinone glycosyltransferase that were induced by SA, two genes, *Pbr014154.1* and *Pbr014155.1*, were also annotated with the function of hydroquinone glycosyltransferase. To further investigate the role of these five genes in the synthesis of arbutin in pear, we detected their expression levels under hydroquinone treatment, and the results are provided in Figure 9. The expression levels of these genes were 5.26-fold, 6.9-fold, 2.29-fold, 4.22-fold, and 5.82-fold higher under hydroquinone treatment compared with the controls, which were not treated with hydroquinone.

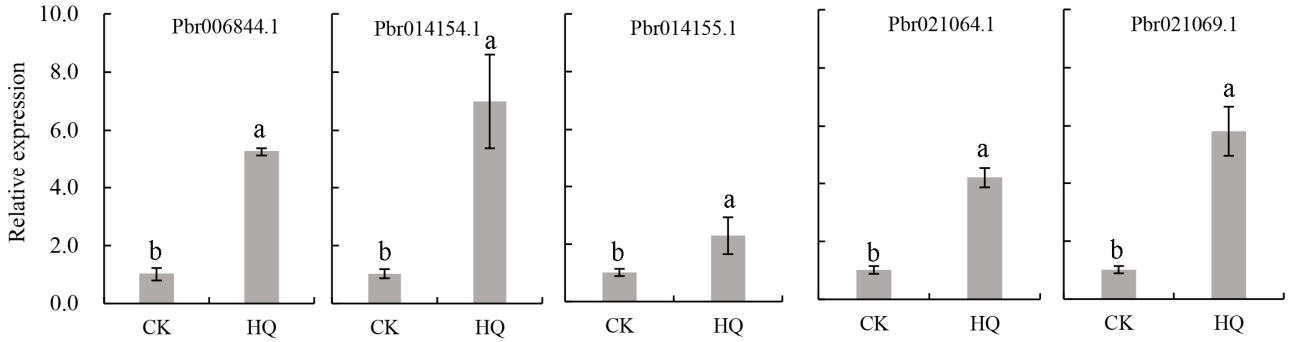

Figure 9. Influence of hydroquinone supply on genes encoding hydroquinone glucosyltransferase ($p < 0.05$). CK = control group, HQ = hydroquinone. The values with different letters indicate significant differences between control and HQ at $p < 0.05$.

3.10. Transient Expression of PbUGT72B1 in Pear Tissue

A heterologous transient expression system was used to research the function of PbUGT72B1 in the synthesis of arbutin in pear. As shown in Figure 10A, after infiltration with GV3101 harboring the pBWA(V)BS-PbUGT72B1 construct, gene transcription was significantly increased with or without hydroquinone. In callus, the introduction of the PbUGT72B1 vector resulted in an increase in arbutin of approximately 35 μg·g^{-1}. When adding hydroquinone, the callus containing the introduced PbUGT72B1 produced 1.83-fold more arbutin compared with the control.

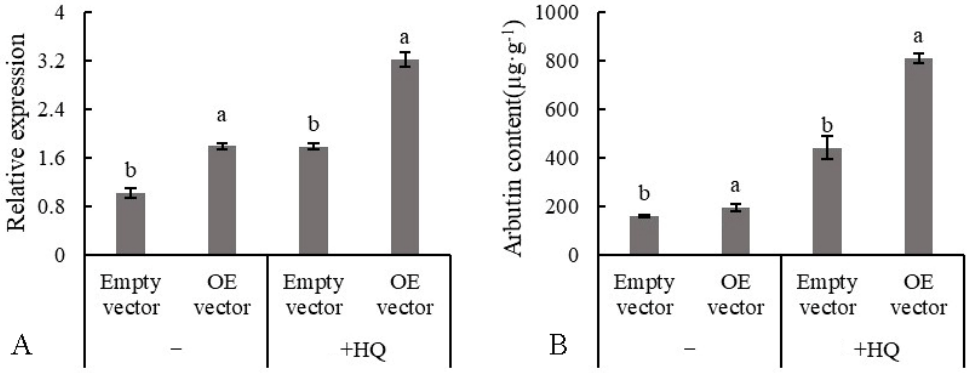

Figure 10. Changes to the arbutin content of callus overexpressing PbUGT72B1. (**A**) Expression level of PbUGT72B1. (**B**) Production of arbutin. OE = overexpression; HQ = hydroquinone. The values with different letters indicate significant differences between empty vector and overexpression vector at $p < 0.05$.

4. Discussion

Fruit is an essential component of a healthy diet. Enhancing the functional and nutritional values of fruit is becoming popular amongst fruit growers to meet consumer demand. Pear is the second most highly consumed pome fruit after apple among adults. Phlorizin is considered to be a special compound specific to apple [6,7]. However, arbutin is a characteristic phenolic glycoside in pear [30], which is different from the phytochemical found in apple. Arbutin is recognized as a medicinal plant substance and a natural compound according to pharmacological experiments [31]. Therefore, it is extremely important to seek technological measures to increase the content of arbutin in pear.

Rafi et al. revealed that EMS (Ethylmethanesulphonate) treatment significantly increases the arbutin content of *Bergenia ciliata* (Haw.) [32]. The effects of GA and ALA treatments on the accumulation of arbutin in pear have also been investigated [33,34]. SA is a signaling molecule used widely in agricultural management activities to regulate plant growth, development, and disease resistance and improve the preservation of fresh agricultural products. Moreover, it is reported to regulate many plant metabolites, including terpene trilactone in *Ginkgo biloba* [23], phenolic acid in *Salvia miltiorrhiza* [35], delphinidin 3-O-glycoside in grape [36], etc. However, there are no published studies that focus on the effect of SA on the content of arbutin in pear. Our findings reveal that the arbutin contents of leaves, fruits, and callus increased after exposure to SA in pear. The results indicate that SA is key to regulating arbutin synthesis.

Transcriptomics offers an efficient approach to unraveling the molecular mechanisms of plant activities. To identify the molecular mechanism that underlies arbutin synthesis, transcriptomic sequencing was performed on pear callus treated with SA. In our transcriptome analysis, 335 DEGs (88.16%) were up-regulated, which is inconsistent with the results reported by Shi et al. To investigate the functions of these DEGs, we carried out a pathway enrichment analysis of these genes using the COG database, which revealed that most were annotated in secondary metabolite biosynthesis, transport, and catabolism (Figure S1). Thirty-three KEGG pathways were identified and, notably, the majority of the up-regulated genes were annotated for phenylpropanoid biosynthesis. These results suggest that SA application changes the secondary metabolic process, consistent with findings reported by Zhang et al. [22]. As early as 1960, Grisdale and Towers found that arbutin is synthesized from phenylpropanoids in pear [17]. The genes encoding phenylalanine ammonia lyase (PAL), cinnamate-4-hydroxylase (C4H), and 4-coumarate: CoA ligase (4CL) are associated with arbutin synthesis [30,37]. In this study, the levels of *PbPAL1*(*Pbr008363.1*), *PbC4H1*(*Pbr013141.1*) and *PbC4H3*(*Pbr017290.1*), *Pb4CL11*(*Pbr036272.1*), and *Pb4CL17*(*Pbr039972.1*) transcription were higher in SA-treated callus. Furthermore, the 1,4-benzoquinone ring precursor may be derived from tyrosine in plants [38]. Ding et al. suggested that some enzymes are associated with hydroquinone synthesis via tyro-

sine metabolism in *Vaccinium dunalianum* Wight [39]. However, we only found one gene (*Pbr008105.1*) to be involved in tyrosine metabolism, indicating that SA mainly regulates phenylpropanoid metabolism, which affects the synthesis of hydroquinone.

Additionally, UDP-glucose, a glucosyl donor, is a substrate involved in the biosynthesis of arbutin. Ten pathways, including starch and sucrose metabolism, amino sugar and nucleotide sugar metabolism, galactose metabolism, etc., were shown to participate in the synthesis of UDP-glucose based on the transcriptome data obtained [39]. In this study, four KEGG pathways related to UDP-glucose synthesis were found, including amino sugar and nucleotide sugar metabolism, pentose and glucuronate interconversion, galactose metabolism, and starch and sucrose metabolism. In starch and sucrose metabolism, sucrose synthase directly accelerates the reversible conversion of sucrose and UDP into UDP-glucose and fructose [40]. However, our results showed that no genes encoding sucrose synthase were induced by SA; therefore, changes in the transcription levels of other genes may affect these metabolic processes.

Arbutin is a hydroquinone glucoside. Glycosylation, catalyzed by glycosyltransferase, is a crucial step in arbutin synthesis. Hydroquinone glucosyltransferase (arbutin synthase, AS) from *R. serpentina*, which is capable of accepting UDPG from glucose as a glucosyl donor to generate arbutin, was the first example of this enzyme to be purified and characterized, and it was used to establish a pathway for the de novo biosynthesis of arbutin [18,19]. Xu et al. (2013) revealed that *PtUGT72B1* from *Populus trichocarpa* could be used to detoxify hydroquinone by glucosylation [41]. Du et al. (2015) cloned a gene encoding AS from *Vaccinium dunalianum* and demonstrated it to be homologous with RSUGT [42]. In a previous study, we identified the members of the UGT family in the pear genome, and *Pbr006844.1*, *Pbr014154.1*, *Pbr014155.1*, *Pbr021064.1*, and *Pbr021069.1* had the closest relationship with the AS gene from *R. serpentina* [43]. In the present study, proteins encoded by the five genes were annotated as hydroquinone glycosyltransferases, and the transcription levels of the genes were increased by adding hydroquinone, similar to results reported by Wu et al. [44]. The data strongly suggest that AS gene expression is regulated by hydroquinone content. Furthermore, among the five genes identified, three were induced by SA, which corresponds well with the arbutin content measured in our experiments, indicating that these three genes participate in the SA-induced regulation of arbutin synthesis.

5. Conclusions

In summary, exogenous SA treatment increased the arbutin content in pear. SA treatment resulted in the up-regulation of 335 transcripts, and most of the DEGs were enriched in metabolism pathways. Six DEGs were involved in the synthesis of hydroquinone and fifteen in the synthesis of UDP-glucose. Fifteen genes related to glycosyltransferase were induced by SA and three DEGs (*Pbr006844.1*, *Pbr021064.1* and *Pbr021069.1*) encoding hydroquinone glucosyltransferase were up-regulated, revealing that they may participate in the final glycosylation step. Furthermore, transient overexpression of *PbUGT72B1* (*Pbr021069.1*) promoted the arbutin content of pear callus. These results provide a theoretical basis for understanding the synthesis of arbutin in plants and offer insights for further research into controlling arbutin biosynthesis and accumulation.

Supplementary Materials: The following supporting information can be downloaded at: https://www.mdpi.com/article/10.3390/horticulturae10060622/s1, Figure S1: COG function classification of the DEGs; Figure S2: Histogram presentation of Gene Ontology classification. The results were divided into three categories, including biological processes, cellular components and molecular functions; Figure S3: KEGG pathway functional annotations for DEGs. Blue column represented organismal systems, green column represented metabolism, pink column represented genetic information processing, purple column represented environmental information processing, and yellow column represented cellular processes; Figure S4: Expression characteristics of 15 genes analyzed by qRT-PCR; Figure S5: Validation of RNA-Seq results using qRT-PCR. P represented Pearson coefficient; Table S1: The primer information of genes; Table S2: The sequence data of RNA-seq; Table S3:

Statistics of functional annotation of pear unigenes; Table S4: The growth rate and arbutin production of callus after feeding with hydroquinone.

Author Contributions: Conceptualization, L.L.; visualization, investigation, J.L., Y.M., T.C. and S.L.; writing—original draft preparation, J.L. and Y.M.; writing—review and editing, J.L. and Y.M.; supervision, project administration, funding acquisition. L.L. All authors have read and agreed to the published version of the manuscript.

Funding: This research was funded by the central leading local science and technology development fund project (Grant No. YDZJSX2022A042), and the biological breeding project of Shanxi Agricultural University (Grant No. YZGC109).

Data Availability Statement: Data are contained within the article and Supplementary Materials.

Acknowledgments: We thank Modern Agriculture Research Center of Shanxi Academy of Agricultural Sciences for providing 1260-HPLC for this experiment.

Conflicts of Interest: The authors declare no conflicts of interest.

References

1. Wu, J.Y.; Fan, J.B.; Li, Q.H.; Jia, L.T.; Xu, L.L.; Wu, X.; Wang, Z.W.; Li, H.X.; Qi, K.J.; Qiao, X.; et al. Variation of organic acids in mature fruits of 193 pear (*Pyrus* spp.) cultivars. *J. Food Compos. Anal.* **2022**, *109*, 104483. [CrossRef]
2. Hong, S.Y.; Lansky, E.; Kang, S.S.; Yang, M. A review of pears (*Pyrus* spp.), ancient functional food for modern time. *BMC Complement. Med. Ther.* **2021**, *21*, 219. [CrossRef] [PubMed]
3. Reiland, H.; Slavin, J. Systematic Review of Pears and Health. *Nutr. Today* **2015**, *50*, 301–305. [CrossRef] [PubMed]
4. Navaei, N.; Pourafshar, S.; Akhavan, N.S.; Litwin, N.S.; Foley, E.M.; George, K.S.; Hartley, S.C.; Elam, M.L.; Rao, S.; Arjmandi, B.H.; et al. Influence of daily fresh pear consumption on biomarkers of cardiometabolic health in middle-aged/older adults with metabolic syndrome: A randomized controlled trial. *Food Funct.* **2019**, *10*, 1062–1072. [CrossRef] [PubMed]
5. Chandel, R.; Kumar, V.; Kaur, R.; Kumar, S.; Kumar, A.; Kumar, D.; Kapoor, S. Bioactive compounds, health benefits and valorization of *Pyrus pyrifolia* (sand pear): A review. *Nutr. Food Sci.* **2023**, *53*, 1061–1080. [CrossRef]
6. Ulaszewska, M.; Vázquez-Manjarrez, N.; Garcia-Aloy, M.; Llorach, R.; Mattivi, F.O.; Dragsted, L.; Praticò, G.; Manach, C. Food intake biomarkers for apple, pear, and stone fruit. *Genes Nutr.* **2018**, *13*, 29. [CrossRef] [PubMed]
7. Fischer, T.C.; Malnoy, M.; Hofmann, T.; Schwab, W.; Palmieri, L.; Wehrens, R.; Schuch, L.A.; Muller, M.; Schimmelpfeng, H.; Velasco, R.; et al. F1 hybrid of cultivated apple (*Malus* × *domestica*) and European pear (*Pyrus communis*) with fertile F2 offspring. *Mol. Breed.* **2014**, *34*, 817–828. [CrossRef]
8. Funayama, M.; Arakaw, H.; Yamamoto, R.; Nishino, T.; Shin, T.; Murao, S. Effects of α- and β-Arbutin on Activity of Tyrosinases from Mushroom and Mouse Melanoma. *Biosci. Biotechnol. Biochem.* **1995**, *59*, 143–144. [CrossRef] [PubMed]
9. Li, X.; Wang, T.T.; Zhou, B.; Gao, W.Y.; Cao, J.G.; Huang, L.Q. Chemical composition and antioxidant and anti-inflammatory potential of peels and flesh from 10 different pear varieties (*Pyrus* spp.). *Food Chem.* **2014**, *152*, 531–538. [CrossRef]
10. Migas, P.; Krauze-Baranowska, M. The significance of arbutin and its derivatives in therapy and cosmetics. *Phytochem. Lett.* **2015**, *13*, 35–40. [CrossRef]
11. Ragab, D.; Salah Eldin, H.; Taeimah, M.; Khattab, R.; Salem, R. The COVID-19 cytokine storm; what we know so far. *Front. Immunol.* **2020**, *11*, 1446. [CrossRef] [PubMed]
12. Nahar, L.; Al-Groshi, A.; Kumar, A.; Sarker, S.D. Arbutin: Occurrence in Plants, and Its Potential as an Anticancer Agent. *Molecules* **2022**, *27*, 8786. [CrossRef]
13. Jurica, K.; Gobin, I.; Kremer, D.; Čepo, D.V.; Grubešić, R.J.; Karačonji, I.B.; Kosalec, I. Arbutin and its metabolite hydroquinone as the main factors in the antimicrobial effect of strawberry tree (*Arbutus unedo* L.) leaves. *J. Herb. Med.* **2017**, *8*, 17–23. [CrossRef]
14. Kuźniak, E.; Wielanek, M.; Chwatko, G.; Głowacki, R.; Libik-Konieczny, M.; Piątek, M.; Gajewska, E.; Skłodowska, M. Salicylic acid and cysteine contribute to arbutin-induced alleviation of angular leaf spot disease development in cucumber. *J. Plant Physiol.* **2015**, *181*, 9–13. [CrossRef] [PubMed]
15. Wei, B.; Hou, K.; Zhang, H.H.; Wang, X.Y.; Wu, W. Integrating transcriptomics and metabolomics to studies key metabolism, pathways and candidate genes associated with drought-tolerance in *Carthamus tinctorius* L. under drought stress. *Ind. Crops Prod.* **2020**, *151*, 112465. [CrossRef]
16. Lawas, L.M.F.; Li, X.; Erban, A.; Kopka, J.; Jagadish, S.V.K.; Zuther, E.; Hincha, D.K. Metabolic responses of rice cultivars with different tolerance to combined drought and heat stress under field conditions. *GigaScience* **2019**, *8*, giz050. [CrossRef] [PubMed]
17. Grisdale, S.K.; Towers, G.H.N. Biosynthesis of Arbutin from Some Phenylpropanoid compounds in *Pyrus communis*. *Nature* **1960**, *188*, 1130–1131. [CrossRef]
18. Arend, J.; Warzecha, H.; Hefner, T.; StÖckigt, J. Utilizing Genetically Engineered Bacteria to Produce Plant-Specific Glucosides. *Biotechnol. Bioeng.* **2001**, *76*, 126–131. [CrossRef]

19. Hefner, T.; Arend, J.; Warzecha, H.; Siems, K.; StÖckigt, J. Arbutin Synthase, a Novel Member of the NRD1β Glycosyltransferase Family, is a Unique Multifunctional Enzyme Converting Various Natural Products and Xenobioticsy. *Bioorg. Med. Chem.* **2002**, *10*, 1731–1741. [CrossRef]
20. Ali, B. Salicylic acid: An efficient elicitor of secondary metabolite production in plants. *Biocatal. Agric. Biotechnol.* **2021**, *31*, 101884. [CrossRef]
21. Cui, K.B.; Shu, C.; Zhao, H.D.; Fan, X.G.; Cao, J.K. Preharvest chitosan oligochitosan and salicylic acid treatments enhance phenol metabolism and maintain the postharvest quality of apricots (*Prunus armeniaca* L.). *Sci. Hortic.* **2020**, *267*, 109334. [CrossRef]
22. Zhang, H.Y.; Liu, F.R.; Wang, J.J.; Yang, Q.R.; Wang, P.; Zhao, H.J.; Wang, J.; Wang, C.; Xu, X.H. Salicylic acid inhibits the postharvest decay of goji berry (*Lycium barbarum* L.) by modulating the antioxidant system and phenylpropanoid metabolites. *Postharvest Biol. Technol.* **2021**, *178*, 111558. [CrossRef]
23. Ye, J.B.; Mao, D.; Cheng, S.Y.; Zhang, X.; Tan, J.P.; Zheng, J.R.; Xu, F. Comparative transcriptome analysis reveals the potential stimulatory mechanism of terpene trilactone biosynthesis by exogenous salicylic acid in Ginkgo biloba. *Ind. Crops Prod.* **2020**, *145*, 112104. [CrossRef]
24. Chen, W.; Wang, Y.; Xu, L.; Dong, J.H.; Zhu, X.W.; Ying, J.L.; Wang, Q.J.; Fan, L.X.; Li, C.; Liu, L.W. Methyl jasmonate, salicylic acid and abscisic acid enhance the accumulation of glucosinolates and sulforaphane in radish (*Raphanus sativus* L.) taproot. *Sci. Hortic.* **2019**, *250*, 159–167. [CrossRef]
25. Shi, H.Y.; Cao, L.W.; Yue, X.U.; Yang, X.; Liu, S.L.; Liang, Z.S. Transcriptional profiles underlying the effects of salicylic acid on fruit ripening and senescence in pear (*Pyrus pyrifolia* nakai). *J. Integr. Agric.* **2021**, *20*, 2424–2437. [CrossRef]
26. Xu, Y.; Huo, L.Y.; Zhao, K.K.; Li, Y.W.; Zhao, X.R.; Wang, H.Y.; Wang, W.L.; Shi, H.Y. Salicylic acid delays pear fruit senescence by playing an antagonistic role toward ethylene, auxin, and glucose in regulating the expression of PpEIN3a. *Front. Plant Sci.* **2023**, *13*, 1096645. [CrossRef] [PubMed]
27. Zhao, J.; Zhang, J.S.; Wang, Y.G.; Feng, W.X.; Xu, W.X. Effects of infection of epiphyte caused fruit rot on defense mechanism in pear fruit callus. *Acta Bot. Boreali Occident. Sin.* **2010**, *30*, 2219–2224.
28. Skrzypczak-Pietraszek, E.; Kwiecien, I.; Pietraszek, J. HPLC-DAD analysis of arbutin produced from hydroquinone in a biotransformation process in *Origanum majorana* L. shoot culture. *Phytochem. Lett.* **2017**, *20*, 443–448. [CrossRef]
29. Cui, T.T.; Li, J.H.; Li, N.; Li, F.; Song, Y.Q.; Li, L.L. Optimization of ultrasonic assisted extraction of arbutin from pear fruitlets using response surface methodology. *J. Food Meas. Charact.* **2022**, *16*, 3130–3139. [CrossRef]
30. Fischer, T.C.; Gosch, C.; Pfeiffer, J.; Halbwirth, H.; Halle, C.; Stich, K.; Forkmann, G. Flavonoid genes of pear (*Pyrus communis*). *Trees* **2007**, *21*, 521–529. [CrossRef]
31. Shang, Y.Z.; Wei, W.P.; Zhang, P.; Ye, B.C. Engineering Yarrowia lipolytica for enhanced production of arbutin. *J. Agric. Food Chem.* **2020**, *68*, 1364–1372. [CrossRef] [PubMed]
32. Rafi, S.; Kamili, A.N.; Ganai, B.A.; Parray, J.A.; Jan, S. Variation in root morphology, enhancement in anti-oxidative enzyme responses and improved arbutin and bergenin levels in *Bergenia ciliata* (Haw.) Sternb. raised in vitro via EMS and gamma irradiations. *Plant Cell Tiss Organ Cult.* **2021**, *145*, 43–57. [CrossRef]
33. Zhang, L.M.; Kamitakahara, H.; Sasaki, R.; Oikawa, A.; Saito, K.; Murayama, H.; Ohsako, T.; Itai, A. Effect of exogenous GA4+7 and BA + CPPU treatments on fruit lignin and primary metabolites in Japanese pear "Gold Nijisseiki". *Sci. Hortic.* **2020**, *272*, 109593. [CrossRef]
34. Cao, X.Y.; Sun, H.L.; Wang, X.Y.; Li, W.X.; Wang, X.Q. ABA signaling mediates 5-aminolevulinic acid-induced anthocyanin biosynthesis in red pear fruits. *Sci. Hortic.* **2022**, *304*, 111290. [CrossRef]
35. Dong, J.; Wan, G.W.; Liang, Z.S. Accumulation of salicylic acid-induced phenolic compounds and raised activities of secondary metabolic and antioxidative enzymes in *Salvia miltiorrhiza* cell culture. *J. Biotechnol.* **2010**, *148*, 99–104. [CrossRef] [PubMed]
36. Gomes, E.P.; Borges, C.V.; Monteiro, G.C.; Belin, M.A.F.; Minatel, I.O.; Junior, A.P.; Tecchio, M.A.; Lima, G.P.P. Preharvest salicylic acid treatments improve phenolic compounds and biogenic amines in 'Niagara Rosada' table grape. *Postharvest Biol. Technol.* **2021**, *176*, 111505. [CrossRef]
37. Zhai, R.; Liu, X.T.; Feng, W.T.; Chen, S.S.; Xu, L.F.; Wang, Z.G.; Zhang, J.L.; Li, P.M.; Ma, F.W. Different Biosynthesis Patterns among Flavonoid 3-glycosides with Distinct Effects on Accumulation of Other Flavonoid Metabolites in Pears (*Pyrus bretschneideri* Rehd.). *PLoS ONE* **2014**, *9*, e91945. [CrossRef] [PubMed]
38. Xu, J.J.; Fang, X.; Li, C.Y.; Yang, L.; Chen, X.Y. General and specialized tyrosine metabolism pathways in plants. *aBIOTECH* **2019**, *1*, 97–105. [CrossRef] [PubMed]
39. Ding, Y.; Xiong, H.; Li, N.; Song, J.; Zheng, Y.L.; Liu, X.Z.; Zhao, P. De novo Transcriptome Sequencing of *Vaccinium dunalianum* Wight to Investigate Arbutin and 6′-O-Caffeoylarbutin Synthesis. *Russ. J. Plant Physiol.* **2017**, *64*, 260–282. [CrossRef]
40. Islam, M.Z.; Hu, X.M.; Jin, L.F.; Liu, Y.Z.; Peng, S.A. Genome-wide identification and expression profile analysis of citrus sucrose synthase genes: Investigation of possible roles in the regulation of sugar accumulation. *PLoS ONE* **2014**, *9*, e113623. [CrossRef]
41. Xu, Z.S.; Lin, Y.Q.; Xu, J.; Zhu, B.; Zhao, W.; Peng, R.H.; Yao, Q.H. Selective Detoxification of Phenols by Pichia pastoris and Arabidopsis thaliana Heterologously Expressing the *PtUGT72B1* from Populus trichocarpa. *PLoS ONE* **2013**, *8*, e66878. [CrossRef] [PubMed]
42. Du, W.; Ding, Y.; Zhu, D.Y.; Yin, J.T.; Liu, X.Z.; Zhao, P. Cloning and Bioinformatics Analysis of *VdAS1* Gene in *Vaccinium dunalianum* (Ericaceae). *Plant Divers. Resour.* **2015**, *37*, 71–77.

43. Li, J.H.; Liu, S.H.; Cui, T.T.; Ding, B.P.; Zhou, Z.Q.; Li, L.L. Identification and Expression Characteristics of UDP-Glycosyltransferase Genes in Pear and Their Correlation with Arbutin Accumulation. *Russ. J. Plant Physiol.* **2022**, *69*, 82. [CrossRef]
44. Wu, B.P.; Cao, X.M.; Liu, H.J.; Zhu, C.Q.; Klee, H.; Zhang, B.; Chen, K.S. UDP-glucosyltransferase PpUGT85A2 controls volatile glycosylation in peach. *J. Exp. Bot.* **2019**, *70*, 925–936. [CrossRef]

Disclaimer/Publisher's Note: The statements, opinions and data contained in all publications are solely those of the individual author(s) and contributor(s) and not of MDPI and/or the editor(s). MDPI and/or the editor(s) disclaim responsibility for any injury to people or property resulting from any ideas, methods, instructions or products referred to in the content.